71. Hashimoto H, Fujioka M, Kinumaki H. Kinki Ambulatory Pediatrics Study Group. An office-based prospective study of deafness in mumps. Pediatr Infect Dis J. 2009;28:173–5.
72. Takahashi M, Asano Y, Kamiya H, Baba K, Ozaki T, Otsuka T, Yamanishi K. Development of varicella vaccine. J Infect Dis. 2008;197:S41–4.
73. Izawa T, Ihara T, Hattori A, et al. Application of a live varicella vaccine in children with acute leukemia or other malignant diseases. Pediatrics. 1977;60:805–9.
74. Asano Y, Nakayama H, Yazaki T, et al. Protection against varicella in family contacts by immediate inoculation with live varicella vaccine. Pediatrics. 1977;59:3–7.
75. Ozaki T. Varicella vaccination in Japan: necessity of implementing a routine vaccination program. J Infect Chemother. 2013;. doi:10.1007/s10156-013-0577-x.
76. Kawabe Y, Sugiyama K, Wada Y, Yamada K. 3-year study for the prevention of perinatal HBV infection under the standard method of the Ministry of Health and Welfare, Japan. Acta Paediatr Jpn. 1989;31:659–62.
77. Komatsu H, Inui A, Sogo T, Hiejima E, Kudo N, Fujisawa T. Source of transmission in children with chronic hepatitis B infection after the implementation of a strategy for prevention in those at high risk. Hepatol Res. 2009;39:569–76.

frontiers in
MICROBIOLOGY

METHODS ARTICLE
published: 11 October 2013
doi: 10.3389/fmicb.2013.00298

Sensitive detection of measles virus infection in the blood and tissues of humanized mouse by one-step quantitative RT-PCR

Shota Ikeno[1,2†], Moto-omi Suzuki[1,3†], Mahmod Muhsen[1], Masayuki Ishige[1], Mie Kobayashi-Ishihara[1], Shinji Ohno[4], Makoto Takeda[5], Tetsuo Nakayama[6], Yuko Morikawa[2], Kazutaka Terahara[1], Seiji Okada[7], Haruko Takeyama[3,4] and Yasuko Tsunetsugu-Yokota[1]*

[1] Department of Immunology, National Institute of Infectious Diseases, Tokyo, Japan
[2] Cooperative Major in Advanced Health Science, Tokyo University of Agriculture and Technology/Waseda University Graduate School of Collaborative Education Curriculum, Tokyo, Japan
[3] Department of Life Science and Medical Bioscience, Graduate School of Advanced Science and Engineering, Waseda University, Tokyo, Japan
[4] Department of Virology, Faculty of Medicine, Kyushu University, Fukuoka, Japan
[5] Department of Virology III, National Institute of Infectious Diseases, Tokyo, Japan
[6] Kitasato Institute for Life Science, Kitasato University, Tokyo, Japan
[7] Division of Hematopoiesis, Center for AIDS Research, Kumamoto University, Kumamoto, Japan

Edited by:
Akio Adachi, The University of Tokushima Graduate School, Japan

Reviewed by:
Takashi Irie, Graduate School of Biomedical Sciences, Hiroshima University, Japan
Masato Tsurudome, Mie University Graduate School of Medicine, Japan
Masae Itoh, Nagahama Institute of Bio-Science and Technology, Japan

***Correspondence:**
Yasuko Tsunetsugu-Yokota, Department of Immunology, National Institute of Infectious Diseases, 1-23-1 Toyama, Shinjuku, Tokyo 162-8640, Japan
e-mail: yyokota@nih.go.jp

† Shota Ikeno and Moto-omi Suzuki have contributed equally to this work.

Live attenuated measles virus (MV) has long been recognized as a safe and effective vaccine, and it has served as the basis for development of various MV-based vaccines. However, because MV is a human-tropic virus, the evaluation of MV-based vaccines has been hampered by the lack of a small-animal model. The humanized mouse, a recently developed system in which an immunodeficient mouse is transplanted with human fetal tissues or hematopoietic stem cells, may represent a suitable model. Here, we developed a sensitive one-step quantitative reverse transcription (qRT)-PCR that simultaneously measures nucleocapsid (N) and human RNase P mRNA levels. The results can be used to monitor MV infection in a humanized mouse model. Using this method, we elucidated the replication kinetics of MV expressing enhanced green fluorescent protein both *in vitro* and in humanized mice in parallel with flow-cytometric analysis. Because our qRT-PCR system was sensitive enough to detect MV expression using RNA extracted from a small number of cells, it can be used to monitor MV infection in humanized mice by sequential blood sampling.

Keywords: measles virus infection, humanized mouse, quantitative RT-PCR, EGFP expression, flow cytometry

INTRODUCTION

Measles, a highly contagious childhood disease caused by the measles virus (MV), affects more than 20 million people each year. MV infection is characterized by a high fever with typical Koplik's spots followed by the appearance of a generalized maculopapular rash, and is often associated with respiratory and neuronal complications (Griffin, 2007). Since the implementation of vaccination programs using an effective live attenuated MV vaccine, global measles deaths have decreased dramatically. Nevertheless, measles is still one of the leading causes of death among young children under the age of 5 years, especially in countries with weak health infrastructures, and approximately 158,000 measles death occurred in 2011 (http://www.who.int/mediacentre/factsheets/fs286/en/). The ongoing global vaccination strategy aims to protect small children at high risk.

The MV vaccine is safe, effective, and inexpensive. Based on its long and successful vaccination history, several groups have taken advantage of reverse-genetics technology to utilize the live attenuated MV vaccine strain as a viral vector to elicit immune responses against foreign antigens from various pathogens, such as Env or Gag of human immunodeficiency virus (HIV; Lorin et al., 2004; Stebbings et al., 2012), hepatitis B surface (S) antigen (Singh et al., 1999; Reyes-del Valle et al., 2009), fusion protein of respiratory syncytial virus (Sawada et al., 2011), and envelope glycoprotein of West Nile virus (Despres et al., 2005; Brandler et al., 2012). MV is a human-tropic virus that uses CD46, signaling of lymphocyte activation molecule (SLAM, CD150), and the recently identified epithelial-cell receptor nectin-4 (PVRL4, see review in Kato et al., 2012) as receptors. To test the immune response against MV-based recombinant vaccines, both MV receptor-transgenic mice (Singh et al., 1999; Lorin et al., 2004; Despres et al., 2005) and non-human primates have been used as animal models (Reyes-del Valle et al., 2009; Brandler et al., 2012; Stebbings et al., 2012).

Although non-human primates are susceptible to MV, and they develop pathologies similar to those that occur in humans, the expense of using monkeys in research limits the number of animals that can be used for studies. To overcome such practical problems, various types of human MV receptor-transgenic mice expressing CD46 or CD150 have been developed (review in

Sellin and Horvat, 2009). Unfortunately, MV infection of all of these human MV receptor-expressing mouse models is severely restricted by the presence of murine type I IFN; to establish MV infection, it is necessary to introduce the IFNα receptor knockout into the MV receptor-transgenic mice, even in strains expressing CD150 driven by a native human promoter (Ohno et al., 2007). The IFNα receptor knockout/CD150 knock-in mouse is highly susceptible to MV infection and reproduces some aspects of MV infection in humans, including immunosuppression (Koga et al., 2010). This makes it a useful mouse model for study purposes. However, one problem is the lack of an initial innate immune response, which may modify the outcome of MV infection. Thus, the model may not truly reflect the outcome in humans.

In the early 2000s, a series of immunodeficient mice were developed that allow efficient transplantation of human cells or tissues; these systems are collectively termed "humanized mice." A large number of studies have described the development of human hematopoietic cells and their immunological functions in humanized mice, and technical modifications have been made for the study of various human diseases (Ito et al., 2012). Currently, humanized mouse systems are widely used as alternatives to non-human primate models, especially for the study of human-tropic infectious diseases such as HIV, human T cell leukemia virus (HTLV), dengue virus, HCV, and EB virus (Akkina, 2013). Of the different humanized mice models, the BM/Liver/Thymus transplanted (BLT) mouse, which is transplanted with human fetal liver and thymus tissue in addition to hematopoietic stem cells (HSCs), is recognized as the model that most closely mimics the human immune response (Wege et al., 2008). However, the use of this model is limited, mainly because of the ethical issues surrounding human fetal organs/tissues.

We have recently established an HIV infection model in NOD/SCID/Jak3null (NOJ) mouse transplanted with human cord blood HSCs (Terahara et al., 2013). To study MV infection in humanized NOJ (hNOJ), we infected an MV vaccine strain (AIK-C) expressing enhanced green fluorescent protein (EGFP) into hNOJ and analyzed the MV-infected cells by flow cytometry. The hNOJ mouse is highly susceptible to MV infection; in that study, we observed that GFP^+ cells were present in systemic lymphoid tissues and bone marrow (BM). Because it is important to assess MV infection kinetics in an animal without sacrificing the infected mouse, we developed a highly sensitive one-step quantitative reverse transcription-PCR (qRT-PCR) system to monitor MV infection in human peripheral blood mononuclear cells (PBMCs) circulating in the blood of humanized mice. In this study, we describe how this monitoring system works and demonstrate that the results obtained reflect the actual frequency of MV-infected cells, as determined by flow cytometry.

MATERIALS AND METHODS

CELL FRACTIONATION OF PBMCs

Peripheral blood mononuclear cells were obtained from human blood samples of healthy volunteers. Samples were collected after obtaining the approval of the institutional ethical committee of the National Institute of Infectious Diseases (NIID; No. 350) and written informed consent from each subject. PBMCs were separated by Ficoll–Hypaque density-gradient centrifugation (Lymphosepal; IBL, Gunma, Japan).

To obtain monocyte-derived dendritic cells (MDDCs), monocytes were enriched from PBMCs using CD14 microbeads (Miltenyi Biotec) and cultured in RPMI 1640 supplemented with 10% fetal bovine serum (FBS), 2 mM glutamine, and antibiotics in the presence of interleukin-4 (IL-4) and granulocyte–macrophage colony-stimulating factor (GM-CSF; both 10 ng/ml, from PeproTech Inc., London, UK) for 1 week. T cells were isolated from CD14-negative PBMCs using the Total T Cell Enrichment Kit (STEMCELL technologies, Vancouver, BC, Canada).

PREPARATION OF RNA

Total RNA was extracted from mouse blood, BM, and spleen of humanized mice, human PBMCs, and Jurkat cells expressing human SLAM (Jurkat/hSLAM) using the RNeasy Mini Kit (QIAGEN, Valencia, CA, USA) or the Total RNA Isolation Mini Kit (Agilent Technologies, Santa Clara, CA, USA).

To prepare a standard of MV RNA, the cDNA encoding measles virus nucleocapsid (N) (MV-N: AB052821) was subcloned into the pBluescript II vector, and then MV-N RNA was produced by *in vitro* RNA transcription using the T7 RiboMAX^{TM} Express Large Scale RNA Production System (Promega, Madison, WI, USA). The RNA product was purified by DNase treatment, followed by phenol–chloroform extraction and ethanol precipitation, according to the protocol supplied by the manufacturer. The final concentration of RNA was measured using an ND-1000 spectrophotometer (Thermo, Waltham, MA, USA).

PREPARATION OF STANDARD TEMPLATE DNA

To prepare a standard template DNA, cDNAs of human CD45 (hCD45: NG_007730) and RNase P (NM_006413) were synthesized from total RNA of CEM cells by reverse transcription (RT)-PCR using SuperScript III RT/Platinum Taq Mix (Invitrogen, Carlsbad, CA, USA). The products were further amplified by PCR using TaKaRa Ex Taq Hot Start Version (TAKARA, Otsu, Shiga, Japan) for hCD45, or AmpliTaq Gold 360 (Applied Biosystems, Carlsbad, CA, USA) for RNase P. These PCR products of hCD45 and RNase P were subcloned into plasmids using the pGeneBLAzer TOPO TA Expression kit (Invitrogen) and pGEM-T (Easy) Vector Systems (Promega), respectively.

REAL-TIME RT-PCR ASSAY

To perform real-time qRT-PCR, SuperScript III Platinum One-Step Quantitative RT-PCR system (Invitrogen) was used according to the manufacturer's instructions. Briefly, each reaction contained 1× reaction mix, ROX reference dye, SuperScript III RT/Platinum TaqMix, 0.2 μM specific primers, and 0.1 μM TaqMan probe. Reactions were performed on an Mx3000P qPCR system (Agilent Technologies). Thermocycling parameters included a RT step at 50°C for 20 min, followed by a DNA polymerase activation step at 95°C for 2 min and 50 PCR cycles (95°C for 20 s, 60°C for 30 s). Threshold cycle (C_t) values were calculated for each reaction; C_t represents the cycle at which a statistically significant increase in the emission intensity of the reporter relative to the passive reference dye is first detected.

For detection of hCD45 mRNA, the following sequences were used: forward primer, 5′-GGA AGT GCT GCA ATG TGT CAT T-3′; reverse primer; 5′-CTT GAC ATG CAT ACT ATT ATC TGA TGT CA-3′; TaqMan probe; 5′-FAM-ACA ACT AAA AGT GCT CCT CCA AGC CAG GTC T-BHQ1-3′ (Hamaia et al., 2001). For detection of RNase P mRNA: forward primer, 5′-AGA TTT GGA CCT GCG AGC G-3′; reverse primer, 5′-GAG CGG CTG TCT CCA CAA GT-3′; TaqMan probe, 5′-FAM-TTC TGA CCT GAA GGC TCT GCG CG-BHQ1-3′ (Kimberly et al., 2005). For detection of MV-N RNA: forward primer, 5′-CGA TGA CCC TGA CGT TAG CA-3′; reverse primer, 5′-GCG AAG GTA AGG CCA GAT TG-3′; TaqMan probe, 5′-FAM-AGG CTG TTA GAG GTT GTC CAG AGT GAC CAG-BHQ1-3′ (Hummel et al., 2006).

GENERATION OF HUMANIZED MICE

Humanized NOD/SCID/JAK3null mice were established as described previously (Terahara et al., 2013). In brief, NOJ mice were transplanted with human HSCs ($0.5–1 \times 10^5$ cells) enriched from human umbilical cord blood cells into the livers of irradiated (1 Gy) newborn mice within 2 days after birth. All mice were maintained under specific pathogen-free conditions in the animal facility at NIID and were treated in accordance with the guidelines issued by the Institutional Animal Care and Committee of NIID.

Human umbilical cord blood was donated by the Tokyo Cord Blood Bank (Tokyo, Japan) after obtaining informed consent. The use of human umbilical cord blood cells was approved by the Institutional Ethical Committees of NIID and the Tokyo Cord Blood Bank. Human HSCs were isolated using the CD133 MicroBeads Kit (Miltenyi Biotec, Bergisch Gladbach, Germany). The purity was approximately 90% as assessed by flow cytometry.

PREPARATION AND INFECTION OF MV

Recombinant wild-type MV (IC323: AB016162) expressing EGFP (IC323-EGFP; Hashimoto et al., 2002) and a recombinant vaccine strain of MV (AIK-C: S58435) expressing EGFP (AIK-C-EGFP; Fujino et al., 2007) were grown in Vero/hSLAM cells. Virus titers were determined by plaque assay using Vero/hSLAM cells.

Jurkat/hSLAM cells were infected with various doses of MV [multiplicity of infection (MOI) = 0.25, 0.05, and 0.01] by incubation at 37°C for 1 h, washed twice with phosphate buffered saline (PBS), and seeded on 24-well plates. Cells were harvested immediately after washing (time 0) or 6, 12, 18, or 24 h later. The harvested cells were either lysed for RNA extraction or analyzed by flow cytometry.

Humanized NOD/SCID/JAK3null mice were challenged intravenously (i.v.) with different doses [200, 2,000, 10,000, or 20,000 plaque-forming units (pfu)] of AIK-C-EGFP. Peripheral blood was obtained from MV-infected hNOJ mice at 3, 5, 7, 10, 14, and 21 days post-infection (p.i.). In some experiments, MV-infected hNOJ mice were sacrificed at day 7 p.i. At the time of sacrifice, peripheral blood, BM, spleen, and mesenteric lymph nodes (MLNs) were harvested, and red blood cells were lysed in ACK buffer (0.15 M NH_4Cl, 1 mM $KHCO_3$, and 0.1 mM EDTA-2Na; pH 7.2–7.4).

FLOW-CYTOMETRIC ANALYSIS OF MV-INFECTED CELLS

PE-conjugated anti-human CD150 (A12) and Pacific Blue-conjugated anti-hCD45 (HI30) monoclonal antibodies (mAbs) were purchased from BioLegend Inc. (San Diego, CA, USA). Cells were stained with these mAbs, fixed with 2% formalin/PBS for 15 min at room temperature, washed, and kept at 4°C prior to flow-cytometric analysis. Dead cells were stained with a LIVE/DEAD Fixable Dead Cell Stain Kit (L34957; Invitrogen). Data were collected using a FACScanto (BD Biosciences, San Jose, CA, USA) and analyzed using the FACSDiva (BD Biosciences) or FlowJo (Tree Star, San Carlos, CA, USA) software.

STATISTICAL ANALYSIS

Non-parametric one-way ANOVA was performed to compare cell type-specific differences in hCD45 and RNase P mRNA expression. Spearman's rank correlation coefficient test was also performed to compare the level of MV-N expression and frequency of MV-infected cells. Prism ver.5 software (GraphPad Software, San Diego, CA, USA) was used for all analyses. $P < 0.05$ was considered statistically significant.

RESULTS

HUMAN-SPECIFIC qRT-PCR SYSTEM FOR THE DETECTION OF MV INFECTION

For the detection of MV infection in clinical specimens, Hummel et al. (2006) established a sensitive qRT-PCR system that used primer and probe sets targeting the MV-N gene. In our humanized mouse model, it is necessary to analyze endogenous mRNA expression in human PBMCs to determine the level of human cell-associated MV infection in mouse blood. We initially assumed that hCD45 expression would be suitable to discriminate human hematopoietic cells from co-existing mouse hematopoietic cells *in vivo*. On that basis, we designed human-specific primer and TaqMan probe sets for hCD45 and compared their usefulness with a primer/probe set for a widely used housekeeping gene, RNase P. RNA was extracted from humanized (hu-mouse) or non-humanized (non-hu-mouse) murine splenocytes, and the level of mRNA was measured by one-step qRT-PCR. Both hCD45 and RNase P primer/probe sets detected mRNA expression of target genes from human PBMCs present in hu-mouse spleen, at similar sensitivities, but neither set detected expression in non-hu-mouse (**Figure 1A**). Thus, both primer/probe sets are human-specific. Next, we enriched $CD14^+$ monocytes and T cells from PBMCs by positive and negative magnetic-bead selection, respectively, and then determined the copy numbers of hCD45 and RNase P in these cell fractions from each of five donors. In **Figure 1B**, the expression levels of hCD45 (left panel) and RNase P (right panel) in monocytes and T cells are depicted relative to the level in each donor's PBMCs. Because RNase P expression was less affected by cell type than CD45 expression ($^*P < 0.05$), in subsequent experiments we exclusively used RNase P primer/probe sets as an endogenous control for mRNA expression.

PARALLEL INCREASE IN THE TIME COURSE OF MV-INFECTED CELL FREQUENCY AND MV-N RNA LEVEL *IN VITRO*

Because wild-type MV mainly utilizes SLAM as the receptor for entry into lymphoid cells (Tatsuo et al., 2000), the kinetics of MV

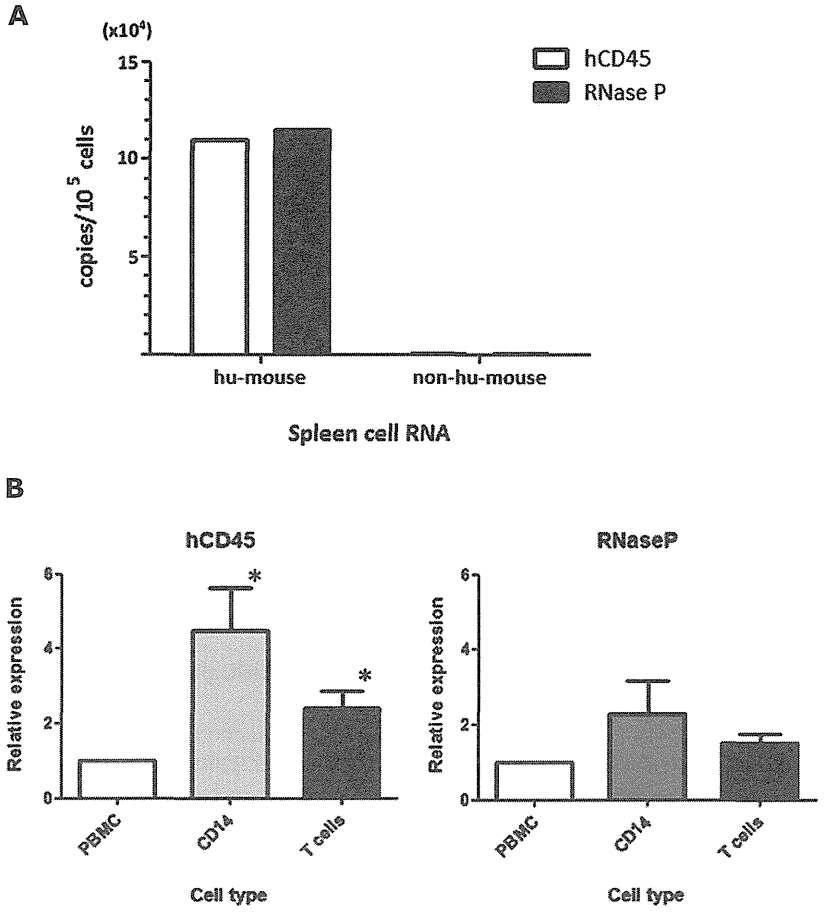

FIGURE 1 | Selection of an endogenous control for the analysis of MV-infected human PBMCs. (A) RNA was extracted from spleen cells of hNOJ and non-humanized NOJ, and one-step qRT-PCR was performed using primer and probe sets designed against the human-specific hCD45 and RNaseP mRNAs. To calculate copy numbers of these genes, the PCR products of human CD45 and RNase P were subcloned into plasmids and used as standard DNAs. **(B)** Human PBMCs from five donors were fractionated into $CD14^+$ monocytes and T cells. RNA from these cell populations was extracted, and the expression levels of hCD45 and RNase P were analyzed by qRT-PCR. The graph depicts the expression levels in these fractionated cells relative to the levels in PBMCs (defined as 1). Statistical differences in hCD45 and RNase P expression among these cell populations were evaluated by non-parametric one-way ANOVA test ($*P<0.05$).

infection in Jurkat/hSLAM cells can be clearly visualized by flow cytometry. We infected Jurkat/hSLAM cells with a wild-type MV encoding EGFP (IC323-EGFP) at MOI of 0.01, 0.05, and 0.25. Cells were washed and harvested at 6, 12, 18, or 24 h after MV infection. A subset of the cells in each sample was analyzed by flow cytometry, and the remainder of the sample was used for RNA extraction. The mRNA levels of MV-N and RNase P were determined by qRT-PCR, and the level of MV-N mRNA relative to RNase P RNA was calculated. Representative results of three experiments are shown in **Figure 2A** (flow cytometry) and **Figure 2B** (qRT-PCR). Because of the rapid and strong cytopathic effect by MV at the highest MOI (0.25), we omitted the flow cytometry data corresponding to that condition. At MOI 0.01, a similar frequency of GFP^+ cells was detectable at 12 and 18 h p.i., whereas at MOI 0.05, the GFP^+ cell frequency was already high at 12 h p.i. Note that the level of hSLAM was not down-modulated by MV infection. Over the time course, relative MV-N expression level at all three MOIs increased in parallel over two orders of magnitude, indicating that these two methods yield comparable results (as shown in **Figure 2C**) and are useful for monitoring the replication kinetics of MV infection *in vitro*.

PARALLEL INCREASE OF MV-INFECTED CELL FREQUENCY AND MV-N RNA LEVELS *IN VIVO*

We then applied these detection systems *in vivo* in MV-infected hNOJ mice. hNOJ mice were infected with an MV vaccine strain expressing EGFP (AIK-C-EGFP) at 2000 pfu, and the animals were sacrificed 7 days later. Blood PBMCs and BM cells were washed with PBS, and a subset of the cells in each sample were stained with anti-hCD45 mAb. Representative results of flow-cytometric analysis of BM cells from three mice are shown in **Figure 3A**. The percentages of GFP^+ cells in mice 127-1, 127-4, and 127-5 mice were low (0.002%), high (0.35%), and intermediate (0.028%), respectively. The number of human PBMCs obtained from mouse blood was not sufficient to determine GFP^+

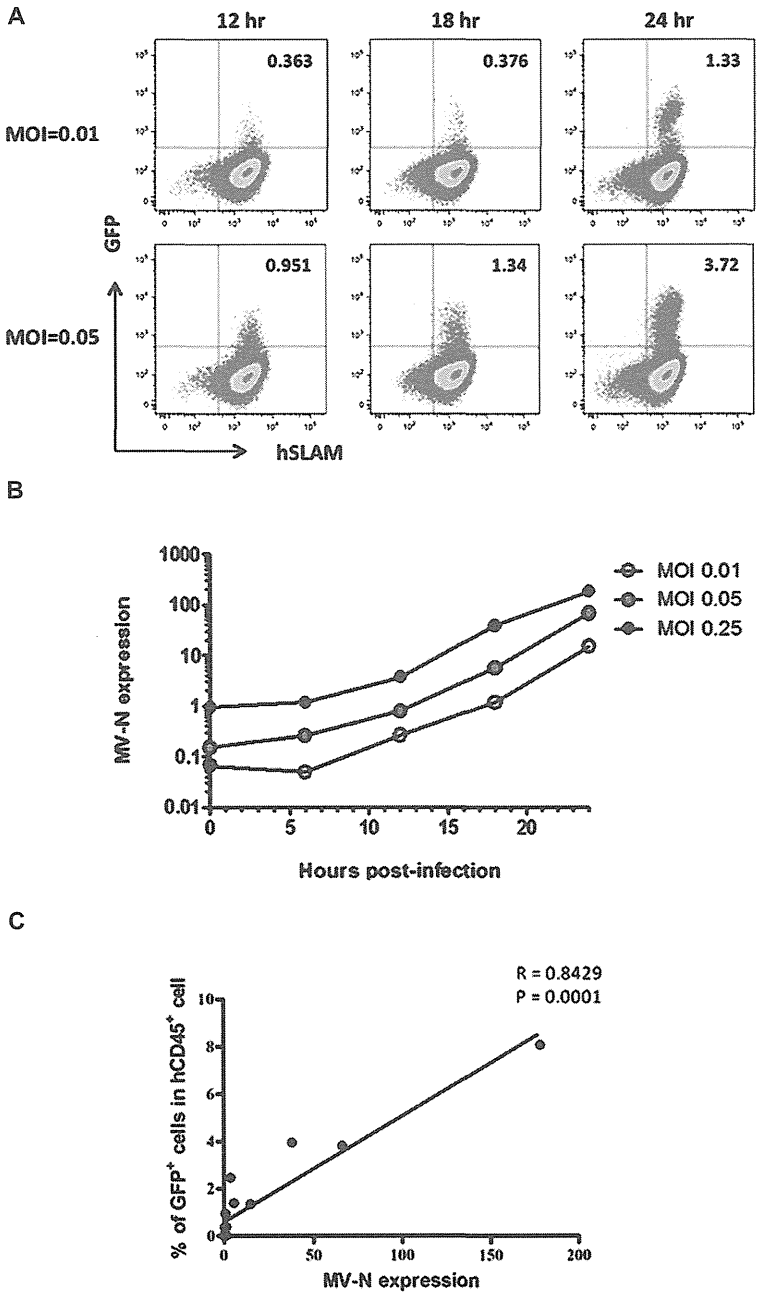

FIGURE 2 | Time course of MV infection *in vitro*. Jurkat/hSLAM cells were infected with wild-type MV IC323-EGFP at MOI of 0.01, 0.05, and 0.25, washed, and harvested at the indicated time points. **(A)** Cells were stained with PE-conjugated anti-hSLAM mAb, fixed with 2% formalin/PBS, and GFP expression was analyzed. **(B)** RNA was extracted from cells, and expression levels of MV-N and RNase P were analyzed by one-step qRT-PCR. The copy numbers of MV-N and RNase P were determined, and the ratio of MV-N copies to RNase P copies is depicted on the vertical axis. **(C)** Correlation between the percentage of GFP^+ Jurkat/SLAM cells and the time course of MV-N expression. Spearman's rank correlation coefficient was used for statistical analysis.

cell frequencies by flow cytometry. Next, we extracted RNA from PBMCs and BM cells and analyzed MV-N expression by qRT-PCR, as described in the previous section. MV-N expression paralleled the GFP^+ frequencies in BM (**Figure 3B**). Notably, a high level of MV-N expression was also detected in PBMCs of mouse 127-4, suggesting that the level of MV-N expression per single hematopoietic cell is similar between blood and BM. We plotted the GFP^+ frequency and MV-N expression level in BM cells of eight mice. As shown in **Figure 3C**, these values were well correlated ($R = 0.9286$). Taken together, these data indicate that MV infection *in vivo* is detectable in BM by both flow cytometry and MV-N RNA qRT-PCR analysis, but only MV-N RNA qRT-PCR is

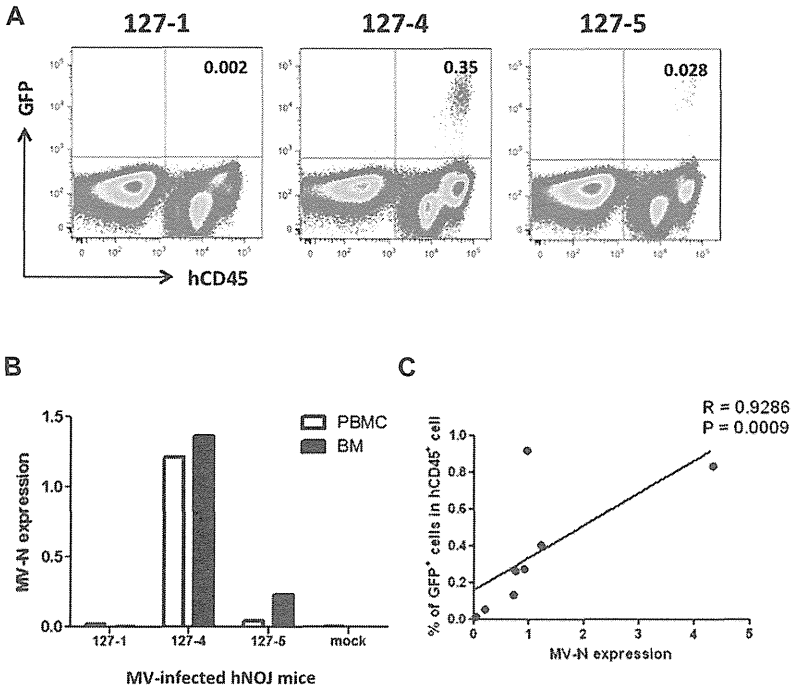

FIGURE 3 | Analysis of MV infection *in vivo*. Three hNOJ mice (127-1, -4, and -5) were infected intravenously with 2,000 pfu of the MV vaccine strain, AIK-C-EGFP. Mice were sacrificed at day 7 post-infection, and blood and bone marrow cells (BM) were obtained. **(A)** BM cells were stained with PB-anti-human CD45 mAb, fixed with 2% formalin/PBS, and GFP expression was analyzed. **(B)** PBMCs from blood and BM cells were lysed, and RNA was prepared. The expression MV-N and RNase P was analyzed as described in the legend for **Figure 2B**. **(C)** Correlation between the percentage of GFP^+ cells among $hCD45^+$ cells in BM and the level of MV-N expression in MV-infected hNOJ mice, at day 7 ($n = 4$) or day 10 ($n = 4$) p.i. Spearman's rank correlation coefficient was used for statistical analysis.

sensitive enough to detect PBMC-associated MV infection in the blood.

KINETICS OF MV GROWTH CAN BE MONITORED IN THE BLOOD OF hNOJ MOUSE

Finally, we measured MV growth kinetics *in vivo* by qRT-PCR analysis using sequential blood samples obtained from MV-infected hNOJ mice; it was not feasible to perform these measurements by flow cytometry because of the paucity of human PBMCs in the blood. Two or three hNOJ mice in each group were infected intravenously with 200, 2000, or 20,000 pfu AIK-C-EGFP and followed up to 21 days p.i. The level of PBMC-associated MV RNA in individual mice is shown in **Figure 4A**. We noticed two peaks of MV replication, the first at around day 3 p.i., and the second at day 10 p.i., irrespective of the initial inoculum. Two mice infected with 20,000 pfu MV exhibited a high level of MV replication that peaked at day 10 p.i. One mouse infected with 2,000 pfu exhibited a high level of MV replication at day 3 p.i., followed by a small peak at day 10 p.i. For some mice, we counted the number of human cells per 50 μl of blood used for RNA extraction. The data are shown in **Figure 4B**. We were able to detect high levels of MV in samples containing less than 2,000 cells, indicating that the qRT-PCR system is sensitive enough to detect low numbers of MV-infected human cells.

Although MV replication was not obvious in three mice infected with the smallest dose (200 pfu), one of these animals exhibited an increase in MV RNA expression at day 21 p.i. (gray circle). We sacrificed this particular mouse and used flow cytometry to analyze GFP expression in its blood, spleen, MLN, and BM. As shown in **Figure 4C**, GFP^+ cells were present in spleen (0.308%) and all the other tissues, albeit at a lower frequency, indicating that MV infection can occur even at a low dose (200 pfu) and spread slowly in the systemic lymphoid tissues of hNOJ.

It may be necessary to acquire at least 30,000 events to be sure of having > 10,000 cells for flow cytometry analysis. This is because of the substantial amount of sample loss that occurs in this system. The flow cytometry data presented in **Figure 4C** were obtained by analyzing ~0.4 ml blood from a sacrificed mouse. However, even under these conditions, the proportion of MV-infected cells detected was only 0.056%; indeed, the cells are barely visible on the plot. Therefore, it appears that flow cytometry is not a suitable method for the sequential monitoring of infected (GFP^+) cells. Thus, the qRT-PCR system we have developed here allowed us to monitor systemic MV replication using a small volume of blood from humanized mice.

DISCUSSION

Based on a highly sensitive MV-N RNA detection method previously developed by Hummel et al. (2006), which could detect one copy of synthetic MV RNA/reaction, we developed a novel one-step real-time qRT-PCR system for the purpose of monitoring MV replication in the blood of MV-infected humanized mice.

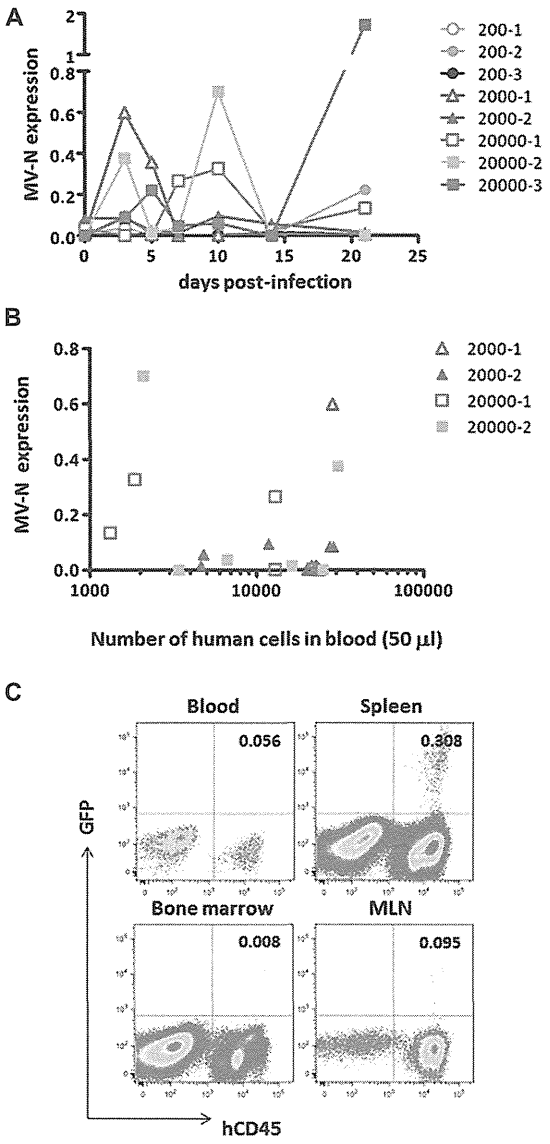

FIGURE 4 | Monitoring of MV replication *in vivo*. Two to three hNOJ mice per group were challenged with MV AIK-C-EGFP at 20,000 (squares), 2,000 (triangles), or 200 pfu (circles). The PBMCs of these mice were collected at day 3, 5, 7, 10, 14, and 21 p.i. **(A)** The level of MV-N expression in the blood of infected hNOJ. Vertical axis shows the level of MV-N relative to that of RNaseP, as described in the legend for **Figure 2B**.**(B)** For some mice (depicted using the same symbol as **(A)**), the number of human cells per 50 µl of blood used for RNA extraction and analyzed for MV-N expression was plotted on the X-axis. **(C)** An hNOJ mouse infected with MV at a low dose (gray closed circle, 200-2) exhibited an increased level of MV-N. At day 21 p.i., the mouse was sacrificed; cells from blood, spleen, BM, and mesenteric lymph node (MLN) were prepared. Cells were stained and analyzed as described in the legend for **Figure 2A**.

Because MV replication usually occurs in association with cells (Griffin, 2007), it is necessary to evaluate the endogenous RNA expression level of human PBMCs that co-exist with mouse blood cells. To this end, we designed human-specific primer/probe sets for the CD45 and RNase P mRNAs. When we analyzed the detection efficiencies of these two primer/probe sets using distinct cell types present in human PBMCs, we found that RNase P expression was less dependent than CD45 expression on cell type. Using this qRT-PCR system with RNase P as an internal control, we can reliably detect MV replication with high sensitivity in humanized mice *in vivo*. When MV expressing GFP was used for infections *in vitro* or *in vivo*, the level of MV-N RNA was closely correlated with the frequencies of GFP^+ MV-infected cells determined by flow cytometry.

Our qRT-PCR system allowed us to follow MV replication *in vivo* using a small amount of blood, with no need to sacrifice mice at each time point. Although flow-cytometric analysis provides valuable information, such as the proportions of various cell types and the surface phenotypes of MV-infected cells, the small number of human cells circulating in the mouse blood may not be sufficient for precise estimation of MV-infected cells by flow cytometry. By contrast, our qRT-PCR system was able to detect MV-N RNA in fewer than 2,000 human PBMCs (**Figure 4B**). This is an important technological advantage considering that individual humanized mice exhibit variable levels of human cell engraftment, i.e., chimerism (Terahara et al., 2013); moreover, there may exist donor-to-donor variation in susceptibility to MV infection. Thus, it should be possible to select humanized mice with a degree of MV infection appropriate for the purpose of a given experiment.

In this study, MV was inoculated through the tail vein, and infected cells were distributed to systemic lymphoid tissues as well as BMs, where human hematopoietic cells localize in humanized mice (Traggiai et al., 2004). MV may also be distributed to other organs, such as lung and intestinal tissue, as demonstrated in the case of HIV infection using the BLT mouse (Sun et al., 2007). To our surprise, by monitoring MV replication in PBMCs of humanized mice, we noticed two peaks of MV replication, at around 3 and 10 days p.i., in some mice. This pattern of MV replication did not depend on the initial dose of MV inoculum. We do not know why MV replication showed two peaks in many animals. However, it was recently reported in a monkey model that MV RNA persists in PBMCs for more than 1 month after primary infection, and declined in three phases (Lin et al., 2012). The authors of that study hypothesized that both T cells, including regulatory T cells (Treg), and antibody responses contributed to the dynamics of MV replication *in vivo*. Although hNOJ mice are reported to show poor immune responses, the role of regulatory T cells should be considered. This is because these cells regulate HIV-1 infection in humanized mice (Jiang et al., 2008). Alternatively, it may be that the intravenous injection of MV rapidly kills the target cells (probably those showing an activated phenotype) within 3 days. The low number of MV-infected cells then gradually transmits the virus to the human cells that are replenished from the BM stem cell pool. Further investigations are required to clarify this issue.

The humanized mouse model is expected to be a useful tool for studying virus infection (Akkina, 2013). Although the human immune system is not fully reconstructed by the transplantation of human HSCs alone, we believe that further improvements are possible, which will allow us to utilize this mouse model to not only evaluate vaccine and drug efficacy but also to increase our understanding of the pathogenesis of MV infection. The described novel method of monitoring MV-infected human cells in the blood will

be useful for studying MV-based vaccines in humanized mouse models without the need to sacrifice the mice.

ACKNOWLEDGMENTS

We thank Prof. Yusuke Yanagi for providing IC323-EGFP, and Ms. Kahori Okano for her excellent technical assistance. We also thank the Tokyo Cord Blood Bank for donating human umbilical cord blood. This work was supported in part by a grant from the Ministry of Health, Labor, and Welfare of Japan, and in part by a grant from the Ministry of Education, Science, Sports, and Culture of Japan. Shota Ikeno is supported by the Global COE Program (Practical Chemical Wisdom) from the Ministry of Education, Culture, Sports, Science, and Technology of Japan.

REFERENCES

Akkina, R. (2013). New generation humanized mice for virus research: comparative aspects and future prospects. *Virology* 435, 14–28. doi: 10.1016/j.virol.2012.10.007

Brandler, S., Marianneau, P., Loth, P., Lacote, S., Combredet, C., Frenkiel, M. P., et al. (2012). Measles vaccine expressing the secreted form of West Nile virus envelope glycoprotein induces protective immunity in squirrel monkeys, a new model of West Nile virus infection. *J. Infect. Dis.* 206, 212–219. doi: 10.1093/infdis/jis328

Despres, P., Combredet, C., Frenkiel, M. P., Lorin, C., Brahic, M., and Tangy, F. (2005). Live measles vaccine expressing the secreted form of the West Nile virus envelope glycoprotein protects against West Nile virus encephalitis. *J. Infect. Dis.* 191, 207–214. doi: 10.1086/426824

Fujino, M., Yoshida, N., Kimura, K., Zhou, J., Motegi, Y., Komase, K., et al. (2007). Development of a new neutralization test for measles virus. *J. Virol. Methods* 142, 15–20. doi: 10.1016/j.jviromet.2007.01.001

Griffin, D. E. (2007). "Measles virus," in *Fields Virology*, eds D. M. Knipe, P. M. Howley, D. E. Griffin, R. A. Lamb, M. A. Martin, B. Roizman, and S. E. Straus, 5 Edn (Philadelphia: Lippincott Williams & Wilkins, a Wolters Kluwer Business), 1551–1585.

Hamaia, S., Li, C., and Allain, J. P. (2001). The dynamics of hepatitis C virus binding to platelets and 2 mononuclear cell lines. *Blood* 98, 2293–2300. doi: 10.1182/blood.V98.8.2293

Hashimoto, K., Ono, N., Tatsuo, H., Minagawa, H., Takeda, M., Takeuchi, K., et al. (2002). SLAM (CD150)-independent measles virus entry as revealed by recombinant virus expressing green fluorescent protein. *J. Virol.* 76, 6743–6749. doi: 10.1128/JVI.76.13.6743-6749.2002

Hummel, K. B., Lowe, L., Bellini, W. J., and Rota, P. A. (2006). Development of quantitative gene-specific real-time RT-PCR assays for the detection of measles virus in clinical specimens. *J. Virol. Methods* 132, 166–173. doi: 10.1016/j.jviromet.2005.10.006

Ito, R., Takahashi, T., Katano, I., and Ito, M. (2012). Current advances in humanized mouse models. *Cell. Mol. Immunol.* 9, 208–214. doi: 10.1038/cmi.2012.2

Jiang, Q., Zhang, L., Wang, R., Jeffrey, J., Washburn, M. L., Brouwer, D., et al. (2008). FoxP3+CD4+ regulatory T cells play an important role in acute HIV-1 infection in humanized Rag2−/−gammaC−/− mice in vivo. *Blood* 112, 2858–2868. doi: 10.1182/blood-2008-03-145946

Kato, S. I., Nagata, K., and Takeuchi, K. (2012). Cell tropism and pathogenesis of measles virus in monkeys. *Front. Microbiol.* 3:14. doi: 10.3389/fmicb.2012.00014

Kimberly, W. T., Zheng, J. B., Town, T., Flavell, R. A., and Selkoe, D. J. (2005). Physiological regulation of the beta-amyloid precursor protein signaling domain by c-Jun N-terminal kinase JNK3 during neuronal differentiation. *J. Neurosci.* 25, 5533–5543. doi: 10.1523/JNEUROSCI.4883-04.2005

Koga, R., Ohno, S., Ikegame, S., and Yanagi, Y. (2010). Measles virus-induced immunosuppression in SLAM knock-in mice. *J. Virol.* 84, 5360–5367. doi: 10.1128/JVI.02525-09

Lin, W. H., Kouyos, R. D., Adams, R. J., Grenfell, B. T., and Griffin, D. E. (2012). Prolonged persistence of measles virus RNA is characteristic of primary infection dynamics. *Proc. Natl. Acad. Sci. U.S.A.* 109, 14989–14994. doi: 10.1073/pnas.1211138109

Lorin, C., Mollet, L., Delebecque, F., Combredet, C., Hurtrel, B., Charneau, P., et al. (2004). A single injection of recombinant measles virus vaccines expressing human immunodeficiency virus (HIV) type 1 clade B envelope glycoproteins induces neutralizing antibodies and cellular immune responses to HIV. *J. Virol.* 78, 146–157. doi: 10.1128/JVI.78.1.146-157.2004

Ohno, S., Ono, N., Seki, F., Takeda, M., Kura, S., Tsuzuki, T., et al. (2007). Measles virus infection of SLAM (CD150) knockin mice reproduces tropism and immunosuppression in human infection. *J. Virol.* 81, 1650–1659. doi: 10.1128/JVI.02134-06

Reyes-del Valle, J., Hodge, G., Mcchesney, M. B., and Cattaneo, R. (2009). Protective anti-hepatitis B virus responses in rhesus monkeys primed with a vectored measles virus and boosted with a single dose of hepatitis B surface antigen. *J. Virol.* 83, 9013–9017. doi: 10.1128/JVI.00906-09

Sawada, A., Komase, K., and Nakayama, T. (2011). AIK-C measles vaccine expressing fusion protein of respiratory syncytial virus induces protective antibodies in cotton rats. *Vaccine* 29, 1481–1490. doi: 10.1016/j.vaccine.2010.12.028

Sellin, C. I., and Horvat, B. (2009). Current animal models: transgenic animal models for the study of measles pathogenesis. *Curr. Top. Microbiol. Immunol.* 330, 111–127. doi: 10.1007/978-3-540-70617-5_6

Singh, M., Cattaneo, R., and Billeter, M. A. (1999). A recombinant measles virus expressing hepatitis B virus surface antigen induces humoral immune responses in genetically modified mice. *J. Virol.* 73, 4823–4828.

Stebbings, R., Fevrier, M., Li, B., Lorin, C., Koutsoukos, M., Mee, E., et al. (2012). Immunogenicity of a recombinant measles-HIV-1 clade B candidate vaccine. *PLoS ONE* 7:e50397. doi: 10.1371/journal.pone.0050397

Sun, Z., Denton, P. W., Estes, J. D., Othieno, F. A., Wei, B. L., Wege, A. K., et al. (2007). Intrarectal transmission, systemic infection, and CD4+ T cell depletion in humanized mice infected with HIV-1. *J. Exp. Med.* 204, 705–714. doi: 10.1084/jem.20062411

Tatsuo, H., Ono, N., Tanaka, K., and Yanagi, Y. (2000). SLAM (CDw150) is a cellular receptor for measles virus. *Nature* 406, 893–897. doi: 10.1038/35022579

Terahara, K., Ishige, M., Ikeno, S., Mitsuki, Y. Y., Okada, S., Kobayashi, K., et al. (2013). Expansion of activated memory $CD4^+$ T cells affects infectivity of CCR5-tropic HIV-1 in humanized NOD/SCID/JAK3^{null} mice. *PLoS ONE* 8:e53495. doi: 10.1371/journal.pone.0053495

Traggiai, E., Chicha, L., Mazzucchelli, L., Bronz, L., Piffaretti, J. C., Lanzavecchia, A., et al. (2004). Development of a human adaptive immune system in cord blood cell-transplanted mice. *Science* 304, 104–107. doi: 10.1126/science.1093933

Wege, A. K., Melkus, M. W., Denton, P. W., Estes, J. D., and Garcia, J. V. (2008). Functional and phenotypic characterization of the humanized BLT mouse model. *Curr. Top. Microbiol. Immunol.* 324, 149–165. doi: 10.1007/978-3-540-75647-7_10

Conflict of Interest Statement: The authors declare that the research was conducted in the absence of any commercial or financial relationships that could be construed as a potential conflict of interest.

Received: 07 August 2013; accepted: 17 September 2013; published online: 11 October 2013.

Citation: Ikeno S, Suzuki M, Muhsen M, Ishige M, Kobayashi-Ishihara M, Ohno S, Takeda M, Nakayama T, Morikawa Y, Terahara K, Okada S, Takeyama H and Tsunetsugu-Yokota Y (2013) Sensitive detection of measles virus infection in the blood and tissues of humanized mouse by one-step quantitative RT-PCR. Front. Microbiol. 4:298. doi: 10.3389/fmicb.2013.00298

This article was submitted to Virology, a section of the journal Frontiers in Microbiology.

Novel Clinical Features of Recurrent Human Respiratory Syncytial Virus Infections

Ikuko Yui,[1]* Motoko Fujino,[2] Akihito Sawada,[3] and Tetsuo Nakayama[3]

[1]*Yui Clinic, Kawasaki, Japan*
[2]*Department of Paediatrics, Saiseikai Central Hospital, Tokyo, Japan*
[3]*Laboratory of Viral Infection I, Kitasato Institute for Life Sciences, Kitasato University, Tokyo, Japan*

Children and elderly individuals are often infected easily and repeatedly with human respiratory syncytial virus (HRSV); however, the features of recurrent infection in the same individual are defined poorly. To clarify the clinical significance of repeated HRSV infections in relation to subgroup epidemiology, this study performed prospective and longitudinal analyses in children with lower respiratory tract infections over 20 consecutive epidemics between 1985 and 2005 at a pediatric outpatient clinic in Kawasaki, Japan. HRSV infections were confirmed by 2 types of reverse-transcription PCR. Samples obtained from patients with repeated infections were subjected to sequence analysis and cloning analysis. A total of 1,312 lower respiratory tract infections observed in 1,010 patients were diagnosed as HRSV infections. Repeated HRSV infections occurred in 208 of the 1,010 patients. Analysis of the patients with repeated infections revealed that children were often infected multiple times even within a single short epidemic. Some patients were re-infected with strains having the same or virtually identical N gene sequences. In patients infected more than 4 times, cloning analysis revealed more frequent dual infections with both subgroups (23.8%). The HRSV-A subgroup caused subsequent homologous infections more frequently than did HRSV-B; furthermore, HRSV-A infections provided no protection from a second homologous infection. In contrast, HRSV-B infections offered significant protection against a second homologous infection. Statistical analysis revealed alleviation of symptoms with a reduced rate of dyspnoeic attacks only in the group re-infected with homologous HRSV-A strains. Thus, this study elucidates new clinical features of recurrent HRSV infection. ***J. Med. Virol.***

KEY WORDS: human respiratory syncytial virus (HRSV); repeated infections; subgroup epidemiology; clinical characteristics

INTRODUCTION

Human respiratory syncytial virus (HRSV), of the family *Paramyxoviridae*, subfamily *Pneumovirinae*, genus *Pneumovirus*, is the leading cause of lower respiratory tract infections in infants and children [Parrott et al., 1973]. All infants experience at least 1 HRSV infection by 2 years of age [Glezen et al., 1986]. Despite the presence of circulatory antibodies against HRSV, recurrent infections in older children and adults occur throughout life, and protective immunity against re-infections is incomplete and brief [Hall et al., 1991]. There are 2 major antigenic subgroups, A (HRSV-A) and B (HRSV-B), and viruses from these subgroups are considered genetically distinct on the basis of sequencing data [Matheson et al., 2006]. Several findings have raised the possibility that antigenic differences between HRSV subgroups may contribute to re-infection, although the results were not conclusive [Mufson et al., 1987]. Both subgroups are subdivided into

Work performed at Laboratory of Viral Infection I, Kitasato Institute for Life Sciences, Kitasato University, Tokyo, Japan.

*Correspondence to: Ikuko Yui, Yui Clinic, 39 Shimohirama, Saiwai-ku, Kawasaki, Kanagawa 212-0053, Japan.
E-mail: ikuko_y@me.com

Accepted 21 August 2013

DOI 10.1002/jmv.23809
Published online in Wiley Online Library (wileyonlinelibrary.com).

several strains or genotypes according to the attachment glycoprotein (G) gene. More than 3 genotypes in each dominant subgroup usually co-circulate in epidemics, with some strains being replaced each year [Hall et al., 1990; Sullender, 2000; Galiano et al., 2005; Matheson et al., 2006]. The difference between genotypes might be considered to play a role in the establishment of re-infections; however, this requires further investigation [Sullender et al., 1998]. A birth cohort study in Kenya observed that 4 of 12 repeated infections recurred with an identical virus within the same short epidemic [Scott et al., 2005]. Furthermore, in a study with adult volunteers, clinical re-infections occurred repeatedly, even when the subjects were infected with the same strain of HRSV-A within a few months after a natural HRSV-A infection [Hall et al., 1991]. From a study of hospitalized children in Finland, no direct evidence of protection against re-infection with a homologous subgroup was found even within a single season [Waris, 1991]. To clarify the clinical characteristics and significance of HRSV re-infection, a prospective and longitudinal analysis of HRSV infections during 20 consecutive epidemics at the same outpatient clinic was conducted.

MATERIALS AND METHODS

Patients and Clinical Specimens

This study was performed at a private pediatric outpatient clinic in Kawasaki, Japan. A pediatrician in the clinic monitored children with symptoms of lower respiratory tract infection prospectively during the period from December 1985 to August 2005. The diagnosis of lower respiratory tract infection was based on major clinical manifestations such as expiratory wheezing, shortness of breath, hoarseness, barking cough with or without inspiratory stridor, deep or wet chest cough, rhonchi, and rales. Duration of fever $\geq$38°C and the existence of respiratory difficulty (retraction, expiratory wheezing, tachypnoea $\geq$50 breath/min, and/or orthopnoea) on the day of visit or during the illnesses were recorded as clinical features by the pediatrician. Nasopharyngeal secretions or nasal swabs were collected from all patients with lower respiratory tract infections, as described previously [Yui et al., 2003]. If an HRSV infection occurred $\geq$14 days after a previous infection or if the 2 infections were determined to involve different subgroups, the event was defined as a separate infection [Hall et al., 1991]. When a patient was diagnosed with HRSV infection for the first time during a visit to the outpatient clinic, this was determined as the first HRSV infection.

Informed consent for participation in this study was obtained from the parents of all the children. The study protocol was approved by the ethics committee of the Kitasato Institute for Life Sciences, Kitasato University.

Detection of HRSV Antigen

From a total of 1,735 clinical specimens, 1,690 were examined immediately for the presence of HRSV antigens with an enzyme-linked immunosorbent assay (ELISA) kit (Ortho Diagnostics, Raritan, NJ), a TestPack RSV enzyme immunoassay (EIA) kit (Abbott Laboratories, North Chicago, IL) or immunochromatography (IC) using ImmunoCard STAT RSV (Meridian Bioscience, Cincinnati, OH). From 1985 to 1986, an ELISA kit was used for direct antigen detection. Then, EIA was performed until December in 2004, when the manufacturer stopped providing the test kit. The IC test was used subsequently (Fig. 1).

RNA Extraction and RT-PCR

Total RNA was extracted directly from respiratory specimens (nasopharyngeal secretions or nasal swabs) using acid guanidinium thiocyanate phenol–chloroform with minor modifications [Yui et al., 2003], as described previously or using the High Pure Viral RNA Kit (Roche Applied Science, Manheim, Germany) according to the manufacturer's instructions. To amplify HRSV-A and HRSV-B simultaneously, an N gene region conserved between the 2 subgroups was selected (Table I). Early in the study, reverse-transcription PCR (RT-PCR) was performed using primer set 1 (Prs1), as described previously [Yui et al., 2003]. Later in the study, an increased number of samples tested negative by PCR using Prs1, although they were positive by EIA and IC. Because HRSV sequence mutation(s) at the position of Prs1 may cause a failure of PCR amplification, another primer set (Prs2) was synthesized (Table I). First-strand cDNA synthesis was carried out using the CN3 primer (for viral RNA) and CCN6 primer (for mRNA). cDNA was amplified by the first PCR using n-F1(+) and n-B1(−), followed by nested PCR using EcoF3′ (+) and NotB3 (−). When an HRSV infection was suspected clinically or epidemiologically, RT-PCR was conducted irrespective of the rapid antigen detection assay (Fig. 1). All RT-PCR procedures were performed according to the protocol described by Kwok and Higuchi [1989]. Every assay was performed with a negative control.

Restriction Fragment-Length Polymorphism

HRSV subgroups were distinguished using restriction fragment-length polymorphisms (RFLP) of the RT-PCR products, as reported previously [Yui et al., 2003]. In brief, the RT-PCR product of HRSV-A was digested with *Bgl*II and that of HRSV-B was digested with *Hae*III. All PCR products were subjected to RFLP, except the clones obtained from the samples selected for cloning.

Nucleotide Sequencing

All the samples obtained from patients with repeated infections were subjected to sequence analysis.

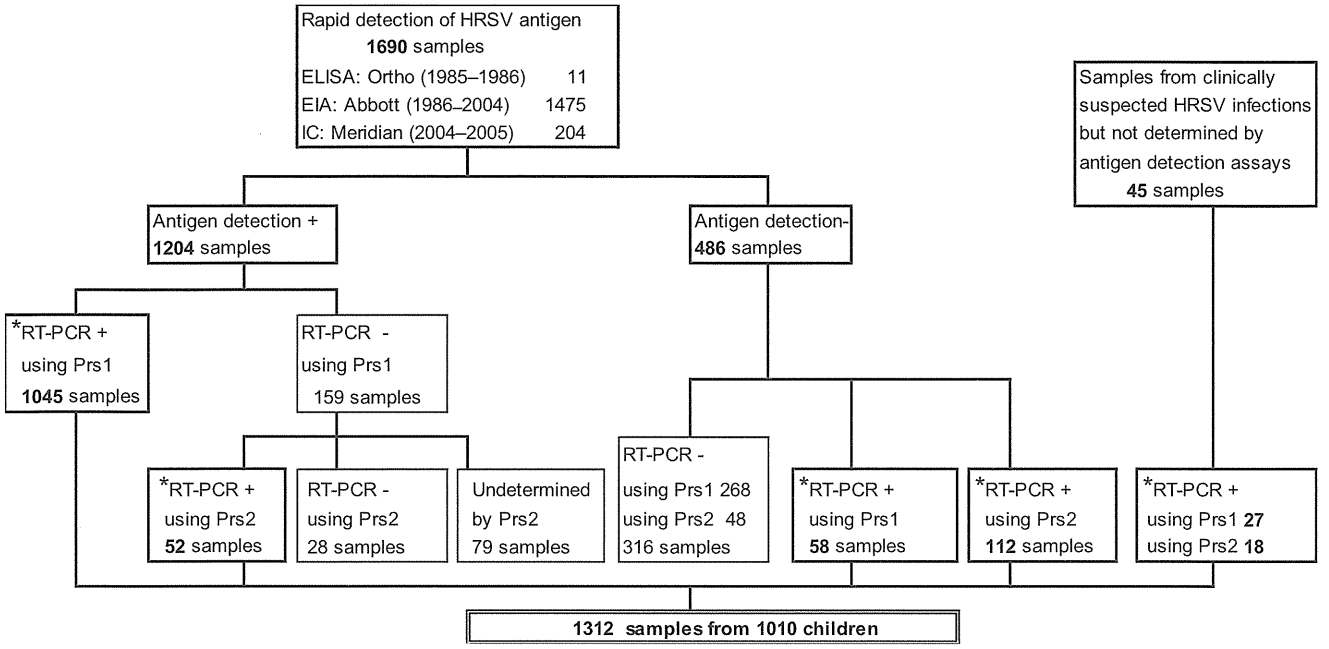

Fig. 1. Study flow diagram. Among the 1,735 clinical specimens, 1,690 were subjected to rapid antigen detection assay and 45 samples from clinically suspected HRSV infections were subjected to RT-PCR. A total of 1,312 specimens obtained from 1,010 children with symptoms of lower respiratory tract infections were confirmed to be infected with HRSV using 2 types of RT-PCR using the primers Prs1 and Prs2. The asterisk represents confirmed HRSV infections. ELISA, enzyme-linked immunosorbent assay; EIA, enzyme immunoassay; IC, immunochromatography; Prs1, RT-PCR primer set 1 shown in Table I; Prs2, RT-PCR primer set 2 shown in Table I.

When a subgroup could not be determined by RFLP due to an atypical cutting pattern, the samples were also subjected to direct sequencing. RT-PCR products were extracted from low-melting-temperature 1% agarose gel and used for sequencing. The nucleotide sequence was determined with a BigDye Terminator v3.1 Cycle Sequencing Kit (Applied Biosystems, Tokyo, Japan) using an automated 3130/3130xl Genetic Analyzer (Applied Biosystems, Foster City, CA). RT-PCR products from samples that were suspected of dual infections of HRSV-A and HRSV-B, based on the RFLP pattern and samples from children infected with HRSV more than 4 times, were inserted into pBluescript II SK (−) (Stratagene, La Jolla, CA); then, nucleotide sequences of more than 20 individual clones from each PT-PCR product were determined

TABLE I. Sequences and Positions of the PCR Primers Used

Primer	Sequence (5′–3′)	Positions
RT-PCR primer set 1 (Prs1)		
C-RSN (+)	GGGTCGACAATTCACTGGGTTAATACCTAT	1274–1295*
RSN-F1 (+)	GCCCCGGGGAGATAGAATCTAGAAAATCCT	1477–1498
RSN-B1 (−)	GCGGAGCTCTTTGGGTTGTTCAATATATGG	1998–2018
RSN-F2 (+)	CCGGTACCGAAATGGGAGAGGTAGCTCC	1516–1535
RSN-B2 (−)	CCGCATGCATAAACCTCAACAACTTGTTCC	1938–1959
RT-PCR primer set 2 (Prs2)		
CN3 (+)	GCTCTTAGCAAAGTCAAGTTGAA	1099–1121*
CCN6 (−)	TCTGTACTCTCCCATTATGCCTA	2087–2109
n-F1 (+)	GAGATAGAATCTAGAAAATCCTACAAAA	1477–1504
n-B1 (−)	TGGGTTGTTCAATATATGGTAGA	1994–2016
EcoF3′ (+)	TGGTGAATTCGCTCCAGAATACAGGCA	1531–1547
NotB3 (−)	AGTTGCGGCCGCATAAACCTCAACAACTTGTTCC	1938–1959
Colony direct PCR primers		
M13m4 (+)	GTTTTCCCAGTCACGAC	580–596**
M13RV (−)	CAGGAAACAGCTATGAC	812–828

The number of nucleotides is based on the genomic location of HRSV-A strain A2* (GenBank accession number M11486) and pBluescript II SK (−)** (GenBank accession number X52330). Underlined letters indicate the linker sequences.

(cloning analysis). A pair of primers, M13m4 (+) and M13RV (−) shown in Table I, was used for colony direct sequencing.

Statistical Analysis

Comparisons between mean values, paired but not normally distributed, were assessed with the Wilcoxon rank sum test. Categorical data were compared by the Chi-square test or Fisher's exact test. All comparisons were conducted at the two-tailed 0.05 level of significance using Stat-View 5.0 software (SAS Institute, Tokyo, Japan).

Nucleotide Sequence Accession Numbers

The N-gene sequences determined in this study have been deposited in the DNA Data Bank of Japan (DDBJ) under accession numbers AB722450–AB723492.

RESULTS

Laboratory Diagnosis of HRSV Infection

Among the 1,735 clinical specimens, 1,690 were subjected to the rapid antigen detection assay, of which 1,204 (71.2%) tested positive for the HRSV antigen (Fig. 1). Early in the study, RT-PCR using Prs1 were conducted. Of the 1,557 samples subjected to RT-PCR using Prs1, 1,130 (72.6%) were positive for HRSV. On comparing the results of EIA and IC to those of RT-PCR, 159 samples were negative by RT-PCR using Prs1, although the viral antigen was detected by EIA or IC (Fig. 1). A portion (80/159) of these samples was re-examined by RT-PCR using another set of primers, Prs2. Using Prs2, 52 samples (65.0%) tested positive for HRSV RNA. Further, of the 486 samples that were negative for antigen detection, 58 and 112 samples were detected to be positive by PCR using Prs1 and Prs2, respectively. Consequently, a total of 1,312 lower respiratory tract infections were confirmed as HRSV infections in 1,010 patients, that is, positive by antigen detection and RT-PCR using Prs1 (1,045) or Prs2 (52), negative by antigen detection but positive by PT-PCR using Prs1 (58) or Prs2 (112), and only detected by RT-PCR using Prs1 (27) or Prs2 (18). The patients ranged in age from 5 days to 11 years (median, 18 months), and the duration analyzed was 20 epidemic years. The definition of 1 epidemic year was from September to August of the next year.

Of the 1,312 HRSV infections, 756 (57.6%) and 517 (39.4%) were caused by HRSV-A and HRSV-B, respectively. Through RFLP and cloning analysis, 39 (3.0%) HRSV infections were verified as dual infections with both HRSV-A and HRSV-B. Further, 617 of 756 (81.6%) HRSV-A infections, 487 of 517 (84.7%) HRSV-B infections, and 20 of 39 (51.3%) infections caused by both HRSV-A and HRSV-B were observed in patients aged less than 3 years. These results showed that HRSV-A and HRSV-B co-circulated continuously over 20 epidemic years, and the overall pattern of subgroup prevalence changed every 1 or 2 years (Fig. 2). From 1994 to 2005, 1 year of HRSV-A predominance was followed by 1 or 2 intervening years where the 2 subgroups presented in similar numbers or HRSV-B predominated.

Rate of Repeated HRSV Infection

From the sequencing and cloning analyses, a total of 208 children were noted to have experienced multiple HRSV infections (2–9 times). Consequently,

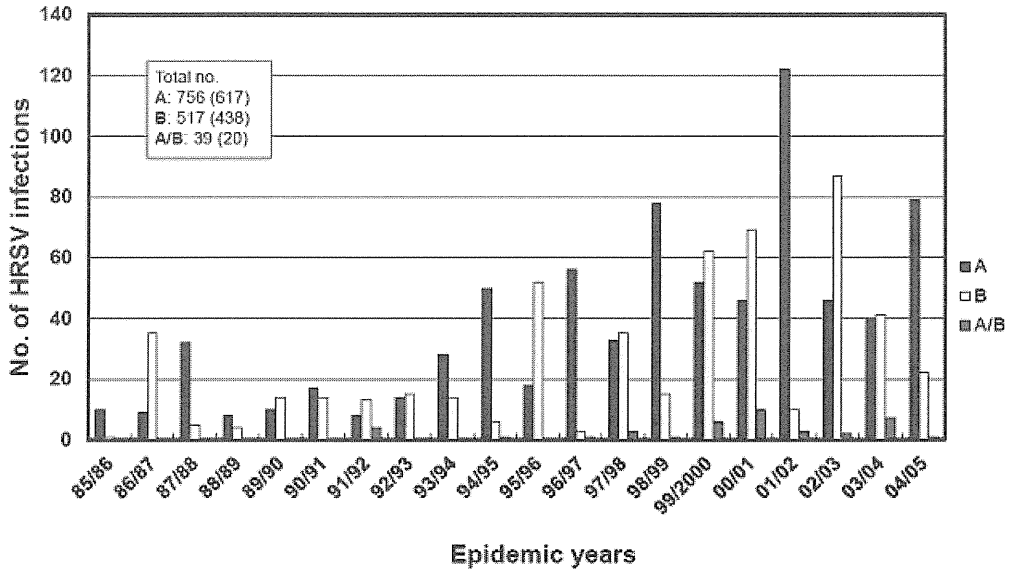

Fig. 2. HRSV subgroup epidemiology. Distribution of HRSV subgroups circulating in Kawasaki, Japan, during 1985–2005. The number in parentheses indicates HRSV infections among patients aged less than 3 years. A, HRSV-A; B, HRSV-B; A/B, dual infection with HRSV-A and HRSV-B.

TABLE II. Patterns of Occurrence Among Children Infected Repeatedly With HRSV

Patterns of occurrence in repeated infections	No. of patients	No. of specimens	HRSV subgroup		
			A	B	A/B
Twice	151	302	186	103	13
Three times	42	126	72	48	6
Four times	6	24	16	4	4
Five times	3	15	8	2	5
Six times	3	18	11	3	4
Eight times	2	16	8	4	4
Nine times	1	9	5	2	2
Total	208	510	306[a]	166[a]	38

[a]Difference between percentages of sample numbers of repeated cases for the total number of HRSV-A and HRSV-B cases is statistically significant ($P = 0.0029$). A/B indicates dual infection with HRSV-A and HRSV-B.

510 infections (510/1,312 = 38.9%) were recorded as multiple infections observed in the 208 children. Among the 510 infections, 306, 166, and 38 infections were caused by HRSV-A, HRSV-B, and both subgroups, respectively (Table II). The rate of repeated HRSV-A infections among the total circulating HRSV-A infections (306/756 = 40.5%) was higher than that of HRSV-B infections (166/517 = 32.1%). The difference in the rate of HRSV-A and HRSV-B infections was statistically significant ($P = 0.0029$). Among the 208 children infected repeatedly with HRSV, 151 and 42 children were re-infected and infected 3 times, respectively. Further, 6, 3, and 3 children were infected 4, 5, and 6 times, respectively. Two children were infected 8 times, and 1 patient was infected 9 times (Table II).

Subgroup Occurrence Among Children Re-Infected With HRSV

During the 20 epidemic years, 151 children experienced HRSV re-infections (302 infections; Table III). The patients had no underlying conditions such as congenital heart disease, immunodeficiencies, neuromuscular disorders, or chronic respiratory disorders, except previously diagnosed asthma (in 10 patients). Five children with low birth weights (<2,500 g) were included in the analysis, as they were not born prematurely, with a gestational age of at least ≥37 weeks. There were 16 (5.3%) cases of hospital admissions (16/302; hospitalization due to the first infection, 12; hospitalization due to a second case of infection, 4) in the group. In the second infection, 60 children were infected with a homologous subgroup, of which 50 and 10 re-infections by a homologous subgroup were caused by HRSV-A and HRSV-B, respectively. Re-infections with a heterologous subgroup were detected in 78 children, of whom 35 and 43 were first infected with HRSV-A and HRSV-B, respectively. Thirteen patients had dual infections with both subgroups in either the first or the second infection. Of the 151 patients, 133 (88.1%) were re-infected after more than 1 season and 18 patients (11.9%) within a single season (Table III). Re-infection with a homologous strain occurred more frequently with HRSV-A than HRSV-B ($P = 0.0065$). During the study period, the overall ratio of circulating HRSV-A/HRSV-B strains in the community was 3:2. Taking circulating HRSV into account, HRSV-A infections provided no protection from a second infection with a homologous strain ($P = 0.91$). However, patients with HRSV-B infections were protected significantly from a second homologous infection

TABLE III. Subgroup Characteristics of HRSV Isolated From Re-Infected Children

Patterns of occurrence	No. of re-infected children	Interval of re-infection				No. of children analyzed for clinical features
		More than 1 separate season		Within a single season		
A–A*	50	43		7		*47*
A–B	35	32		3		*33*
B–B	10	9		1		*9*
B–A	43	39		4		*40*
A/B	13	10	First (5), Second (5)	3	First (2), Second (1)	
Total	151	133		18		*129*

*The first letter designates the subgroup responsible for the first HRSV infection, and the second letter, that for the second infection. A/B indicates that dual infection with both subgroups is included in the first or second infection. The numbers in parentheses indicate dual-infected HRSV samples in the first or second infection. The numbers in italics indicate re-infected children who were enrolled for the analysis of clinical features.

($P = 0.002$). When the comparison was applied to children aged less than 3 years (total number of patients, 91; age range, 1–36 months; median, 15 months), the protection offered by HRSV-B against a second homologous infection was verified ($P = 0.005$). Sequence analysis indicated that 8 children were re-infected with an HRSV-A strain possessing the same nucleotide sequence in the N gene region (nucleotide positions 1548–1937); further, 4 children were infected with an HRSV-A strain and 1 child was infected with an HRSV-B strain possessing a very similar sequence in the N gene region (differing only in a single synonymous nucleotide substitution). The clinical features of 129 children could be traced (Table III).

Subgroup Occurrence Among Children Infected 3 Times

During the study period, 42 children were infected with HRSV 3 times (126 infections; Table IV). Among these, all possible patterns of occurrence were observed. The patients had no underlying conditions except previously diagnosed asthma (in 8 patients) and a low birth weight (in 2 patients). Overall, hospitalization was required in 9 of 126 cases of infections (7.1%; first infection, 6; second infection, 2; third infection, 1). Among the 42 children, 19 (17 + 2) (45.2%) had experienced HRSV infections multiple times (2 or 3 times) within a single epidemic year. The clinical characteristics of 29 children were analyzed (Table IV).

On comparing the first and second infections among patients infected 3 times, the number of patients infected from HRSV-A to HRSV-A (A–A), from HRSV-B to HRSV-B (B–B), from HRSV-A to HRSV-B (A–B), and from HRSV-B to HRSV-A (B–A) were 8, 3, 7, and 11, respectively. Similarly, on comparing the first and third infections, there were 11 (A–A), 2 (B–B), 4 (A–B), and 12 (B–A) children in the various subgroup infection patterns. Likewise, on comparing the second and third infection, 14 (A–A), 1 (B–B), 5 (A–B), and 9 (B–A) children were classified into the various subgroup infection patterns (Table V). Taking circulating HRSV into account, comparisons among the first and second, the first and third, and the second and third homologous infections revealed that HRSV-A or HRSV-B infections conferred no immunity against the same subgroup. However, considering all the patients, independent of the temporal patterns of repetition, HRSV-B infections provided significant protection from a second infection by a homologous strain ($P = 0.003$). Similarly, HRSV-B infections in children aged less than 3 years (total number of patients, 15; age range, 2–36 months; median, 17 months) also provided significant protection against another homologous infection ($P = 0.003$).

Clinical Features Among Children Re-Infected and Infected 3 Times

To assess the alleviation of clinical symptoms in the second or third infection among children re-infected or infected 3 times, the mean number of febrile days and respiratory difficulty were compared between the first and second infections, the first and third, and the second and third infections (Table V).

Among the re-infected patients, a reduction in dyspnoeic attack rates was observed between the first and second HRSV-A infections ($P = 0.004$) (Table V).

TABLE IV. Subgroup Characteristics of HRSV Isolated From Children Infected 3 Times

		Interval of repeated infection 3 times					
Patterns of occurrence	No. of children infected 3 times	More than one separate season		Two infections within a single season		Three infections within a single season	No. of children analyzed for clinical features
A–A–A*	5	2		2		1	*4*
A–A–B	4	1		2	A–A (2)[a]	1	*4*
A–B–A	8	5		3	A–B (2), B–A (1)	0	*7*
A–B–B	1	1		0		0	*0*
B–B–B	2	1		1		0	*1*
B–B–A	3	1		2	B–A (2)	0	*2*
B–A–B	3	2		1	A–B (1)	0	*1*
B–A–A	10	7		3	B–A (3)	0	*10*
A/B	6	3	First (1)[b], Second (2)	3	Second (1), Third (2)	0	
Total	42	23		17		2	*29*

*The first letter designates the subgroup responsible for the first infection; the second letter, that for the second infection; and the third letter, that for the third infection. A/B indicates dual infection in the first, second, or third infection. The numbers in parentheses indicate the sample numbers for each pattern of occurrence in 2 infections within a single season[a], and dual-infected HRSV samples in the first, second, or third infection[b]. The numbers in italics indicate children infected 3 times who were enrolled for the analysis of clinical features.

TABLE V. Comparison of Clinical Features Among Children With HRSV Re-Infection and Who Were Infected 3 Times

	Re-infection					Repeated infection 3 times				
		Fever		Dyspnoea			Fever		Dyspnoea	
Patterns of occurrence	No. of children	Mean no. of febrile days ± SD	*P*-Value	Rate of dyspnoea	*P*-Value	No. of children	Mean no. of febrile days ± SD	*P*-Value	Rate of dyspnoea	*P*-Value
A–A*	47	F = 2.1 ± 0.3 S = 2.1 ± 0.3	0.95	F = 28/47** S = 14/47	0.004	33 (8, 11, 14)	Fs = 1.1 ± 0.3 St = 1.6 ± 0.3	0.23	Fs = 16/33 St = 20/33	0.45
B–B	9	F = 2.4 ± 0.6 S = 2.6 ± 0.6	0.89	F = 5/9 S = 7/9	0.61	6 (3, 2, 1)	Fs = 1.8 ± 0.9 St = 1.0 ± 0.7	0.58	Fs = 2/6 St = 2/6	>0.99
A–B	33	F = 2.4 ± 0.3 S = 1.9 ± 0.3	0.31	F = 16/33 S = 16/33	>0.99	16 (7, 4, 5)	Fs = 0.7 ± 0.3*** St = 2.1 ± 0.5	0.04	Fs = 7/10 St = 4/10	0.46
B–A	40	F = 2.1 ± 0.3 S = 2.5 ± 0.3	0.26	F = 24/40 S = 21/40	0.5	32 (11, 12, 9)	Fs = 2.6 ± 0.3 St = 1.7 ± 0.3	0.33	Fs = 15/32 St = 15/32	>0.99
Total	129					87 (29 × 3)				

*The first letter designates the subgroup responsible for the first HRSV infection (in the re-infection) or the second infection (in the repeated infection 3 times); and the second letter, that for the second (re-infection) or third infection (repeated infection 3 times). The letter "F" indicates the first HRSV infection, "S" and "s" indicate the second, and "f" and "t" indicate the third infection. The numbers in parentheses indicate the number of patients between the first and second infection, the first and third, and the second and third, respectively. The Wilcoxon rank-sum test was used for comparing the mean duration of fever in each infection, and Fisher's exact test or Chi-square test was used for comparing the rate of dyspnoea at each infection. **, ***The differences are statistically significant.

Other homologous or heterologous subgroup re-infections were not significantly different for these clinical characteristics even on comparing the infections occurring at an interval of more than 1 epidemic or within a single epidemic. Similarly, a reduction in dyspnoeic attack rates was observed between the first and second HRSV-A infections in the younger age groups (≤3 years; $P = 0.016$). In contrast, when the younger age groups (≤3 years) infected with HRSV-B were re-infected with HRSV-A, an increase in the number of febrile days was observed.

Among patients infected repeatedly 3 times, all the patients were summed up according to the temporal patterns of repetition (i.e., the first and second, the first and third, and the second and third infections). The alleviation of clinical symptoms was compared among all the patients with these 4 infection patterns (i.e., A–A, B–B, A–B, and B–A; Table V). No significant alleviation of clinical symptoms, such as the duration of fever or rate of dyspnoea, was observed in any of the 4 patterns of occurrence. On the contrary, the mean duration of fever in the infecting pattern from HRSV-A to HRSV-B (A–B) was longer in the second or third infection ($P = 0.04$). The alleviation of these symptoms was not verified; however, the number of febrile days was increased in children belonging to the younger age groups who were infected with HRSV-B after infection with HRSV-A.

Clinical Course of Children Infected More Than 4 Times

Fifteen children were diagnosed with HRSV infections more than 4 times. Among these 15 children, 6, 3, 3, and 2 patients as well as 1 patient had a history of HRSV infections 4, 5, 6, 8, and 9 times, respectively. Consequently, 82 HRSV infections were observed in these 15 children. The patients had no underlying conditions, including previously diagnosed asthma and a low birth weight. There were five (6.1%) hospital admissions (5/82; hospitalization due to the first infection, 4; hospitalization due to second infection, 1). The patients' ages ranged from 1 month to 11 years (median, 31.5 months).

All the infections, except 2, were subjected to cloning analysis, which indicated that 19 infections (23.8%) were dual infections of HRSV-A and HRSV-B. Various random patterns of occurrence were observed in the repeated infections. All 15 children had experienced HRSV infections multiple times within the same epidemic season, and 4 of the 15 children showed 3–5 separate as well as different subgroup infections within a single season. However, there was no apparent decrease in the duration of fever for each infective episode in these patients. On the other hand, respiratory difficulties tended to recur even after multiple infections in 9 of the 15 children. The remaining children had showed no dyspnoeic attacks from the very first infection.

DISCUSSION

This study was conducted in an ambulatory care setting but not with birth cohort monitoring. Previous studies have demonstrated that over two-thirds of children were infected with HRSV within their first year of life [Glezen et al., 1986]. It was also reported that several neonates were completely asymptomatic although infected with HRSV [Hall et al., 1979]. Therefore, it is likely that a considerable number of the patients in this study had already experienced HRSV infections before their first symptomatic episode. Nevertheless, the data in this study showed that HRSV lower respiratory tract infections occurred repeatedly in the same individual at a rate of 20.6% (208/1,010), which was higher than those reported by 2 previous studies as 9.0% and 7.8% [Zlateva et al., 2007; Yamaguchi et al., 2011]. The higher rate of detection of recurrent HRSV infections in this study as compared to those in previous studies may be attributed partly to the differences in the detection methods used. Two different RT-PCR primer sets (Prs1 and Prs2) and antigen detection assays were used in this study, whereas in the other report, HRSV infections were detected using a single RT-PCR protocol targeting the G gene, which is more variable than the N gene targeted by the present RT-PCR protocols [Yamaguchi et al., 2011]. In fact, the first RT-PCR (Prs1) failed to detect a substantial number of HRSV infections, which were identified by the second RT-PCR (Prs2) and antigen detection assays. The present analysis supports the need to identify HRSV infections using more than 2 diagnostic methods, since the number of infections might otherwise be overlooked. These data thus demonstrated that repeated HRSV infections occur more frequently in Japan than indicated by the previous study.

From 1994 to 2005, a cyclic pattern of subgroup prevalence was observed in the present study. Each HRSV-A predominant year was followed by 1 or 2 epidemic years with relatively equal proportions of the 2 subgroups or HRSV-B predominance. Similar cyclic patterns have been reported in Belgium [Zlateva et al., 2007] and in Rochester, New York [Hall et al., 1990]; however, the patterns differed among the reports. The former study was performed using 2 kinds of RT-PCR procedures and the latter using an immunofluorescent test with monoclonal antibodies. Epidemiological studies around the world have disclosed HRSV-A predominance [Sullender, 2000]. However, the high total HRSV-B detection rate of 44% in Zlateva's study compared with 39% in this study; the 29% HRSV-B detection rate in Hall's study might be due to the methods used and/or the appropriate selection of RT-PCR primers for HRSV-B, since HRSV-B has greater variability in terms of stop codon usage and insertion or deletion than does HRSV-A [Matheson et al., 2006]. Therefore, the different detection rates for HRSV-B using various procedures could influence the results of molecular epidemiology.

In this study, no significant difference was observed in the rate of repeated HRSV-A infections by a homologous subgroup as compared with those by a heterologous subgroup. A birth-cohort study conducted over 2 consecutive years showed that re-infections with the same strain possessing the G gene sequence occurred in infants even within the same epidemic year [Scott et al., 2005]. This observation is thus consistent with the data recorded in the present study. In addition, this study confirmed that the rate of re-infection with HRSV-A was higher than that with HRSV-B, which has also been shown previously [Yamaguchi et al., 2011]. Importantly, HRSV-B re-infection provided protection from a second infection with a homologous subgroup among the re-infected children and among the children infected with HRSV 3 times, even on comparison with children from the younger age groups ($\leq$3 years). This might reflect the 2 distinct lineages of divergent evolution with extensive genetic and serologic differences between HRSV-A and HRSV-B [Matheson et al., 2006]. In addition, this might also explain the cyclic pattern of subgroup prevalence.

Many children who suffered from multiple infections within a short period of time were observed in this study; some of these were infected more than 3 times within the same season, suggesting that some individuals, such as children infected more than 4 times, are highly susceptible to HRSV. Individual host genetic factors are considered important to the immunopathogenesis of HRSV infections [Miyairi and DeVincenzo, 2008; Oshansky et al., 2009]. This influence involves a complex interaction of age-related immunity, previous HRSV experience on priming immune-developmental genetic processes, genes protecting against viral entry in the early phase, and genes modifying later immunopathology. The results in the present study might reflect the differences among individual host genetic factors that determine the susceptibility to HRSV. For highlighting the importance of host genetic factors, patients with multiple HRSV infections appeared to be roughly divisible into 2 groups; those suffering dyspnoeic attacks even after many HRSV infections, and those with no respiratory difficulties from the start. The clinical features of patients presenting with recurrent dyspnoeic attack after HRSV infections could possibly be diagnosed with asthma later in their clinical course.

A previous study showed that the incidences of lower respiratory tract infections, bronchiolitis, and otitis media with effusion were reduced on the third but not second infection of HRSV, and that age at infection influenced the disease severity [Henderson et al., 1979]. The clinical features of repeated HRSV infections, such as the number of febrile days and the presence of dyspnoea, were compared among individuals. In addition, these clinical features were compared among

individuals infected with the different subgroups; this analysis was not performed in the previous studies. Among children infected repeatedly with homologous or heterologous HRSV, a reduction in neither the febrile period nor the rate of respiratory difficulty was observed at the second or third infection, even on comparison with children from the younger age group (≤3 years). The only difference noted was a reduced rate of dyspnoeic attacks among the group re-infected with the same HRSV-A, which might indicate that individuals in this group showed a lower immunopathologic response to HRSV-A than the individuals in the other group. In contrast, among the patients infected 3 times, a longer duration of febrile period was noted in the second infection, with infection from HRSV-A to HRSV-B, as compared with the first infection. Similarly, among the re-infected younger age group, infection from HRSV-B to HRSV-A was associated with a longer duration of febrile period. HRSV can occur together with other respiratory viruses, especially adenoviruses [De Paulis et al., 2011]. Although it is possible that other microorganisms modulated the clinical manifestations of HRSV infections at least in some patients in this study, it has been previously reported that viral co-infections do not appear to affect the severity of HRSV infections in hospitalized infants [De Paulis et al., 2011].

The cloning procedure was applied mainly to samples obtained from children with multiple HRSV infections; therefore, a high rate (23.8%) of dual infections was identified. The total rate of dual infections was 3.0%, which was still a relatively high rate of incidence as compared to that reported by an earlier study (0.6%) [Zlateva et al., 2007]. It is possible that more dual infections could be detected by applying cloning procedures to all the samples. The sequence of HRSV-B displays greater variability than that of HRSV-A, which could lead to lower detection rates for HRSV-B and affect the discovery of dual infections, if the primers used to detect HRSV-B are not appropriate for the prevalent strains. It would be worthwhile to examine the exact incidence of dual infections, the manner in which individual clinical symptoms are affected by dual infections, and the evolutionary interaction of HRSV-A and HRSV-B inside the human body.

Recently, it was demonstrated that severe fatal lower respiratory tract infections caused by HRSV are characterized by the absence of a pulmonary cytotoxic lymphocyte response, robust viral loads, and an apoptotic crisis, based on an analysis of autopsy specimens from Chilean infants in the absence of mechanical ventilation [Welliver et al., 2007]. This has cast some doubt on the immunopathogenesis of HRSV disease. The results of the present study may provide additional insights into the wide variations in the severity of HRSV disease, which are affected by the age at infection as well as by genetic polymorphisms among races, individual host genetic factors and socioeconomic conditions [Miyairi and DeVincenzo, 2008; Oshansky et al., 2009]. The susceptibility to HRSV and the disease severity or pattern may vary and depend upon individual factors. If certain genetic factors can predict HRSV disease severity, these findings can lead to either a new vaccination strategy that induces the formation of antibodies blocking the CX3C–CX3CR1 interaction of G protein [Zhang et al., 2010] or antiviral compounds derived from plant lectins [Ooi et al., 2010] as an individualized treatment option.

ACKNOWLEDGMENTS

The authors thank Dr. Yoshinao Takeuchi for many helpful discussions and his critical comments on the original version of the manuscript. The authors also thank Dr. Kouji Kurauchi for his assistance in statistical analysis, Ms. Yoshie Motegi for her skilled technical assistance and Ms. Emiko Mori for her assistance with collecting clinical samples.

REFERENCES

De Paulis M, Gilio AE, Ferraro AA, Ferronato AE, do Sacramento PR, Botosso VF, de Oliveira DB, Marinheiro JC, Hársi CM, Durigon EL, Vieira SE. 2011. Severity of viral coinfection in hospitalized infants with respiratory syncytial virus infection. J Pediatr (Rio J) 87:307–313.

Galiano MC, Palomo C, Videla CM, Arbiza J, Melero JA, Carballal G. 2005. Genetic and antigenic variability of human respiratory syncytial virus (groups A and B) isolated over seven consecutive seasons in Argentina (1995–2001). J Clin Microbiol 43:2266–2273.

Glezen WP, Taber LH, Frank AL, Kasel JA. 1986. Risk of primary infection and reinfection with respiratory syncytial virus. Am J Dis Child 140:543–546.

Hall CB, Kopelman AE, Douglas RG Jr, Geiman JM, Meagher MP. 1979. Neonatal respiratory syncytial virus infection. N Engl J Med 300:393–396.

Hall CB, Walsh EE, Schnabel KC, Long CE, McConnochie KM, Hildreth SW, Anderson LJ. 1990. Occurrence of groups A and B of respiratory syncytial virus over 15 years: Associated epidemiologic and clinical characteristics in hospitalized and ambulatory children. J Infect Dis 162:1283–1290.

Hall CB, Walsh EE, Long CE, Schnabel KC. 1991. Immunity to and frequency of reinfection with respiratory syncytial virus. J Infect Dis 163:693–698.

Henderson FD, Collier AM, Clyde WA Jr, Denny FW. 1979. Respiratory syncytial-virus infections, reinfections and immunity: A prospective, longitudinal study in young children. N Engl J Med 300:530–534.

Kwok S, Higuchi R. 1989. Avoiding false positives with PCR. Nature 339:237–238.

Matheson JW, Rich FJ, Cohet C, Grimwood K, Huang QS, Penny D, Hendy MD, Kirman JR. 2006. Distinct patterns of evolution between respiratory syncytial virus subgroups A and B from New Zealand isolates collected over thirty-seven years. J Med Virol 78:1354–1364.

Miyairi I, DeVincenzo JP. 2008. Human genetic factors and respiratory syncytial virus disease severity. Clin Microbiol Rev 21:686–703.

Mufson MA, Belshe RB, Orvell C, Norrby E. 1987. Subgroup characteristics of respiratory syncytial virus strains recovered from children with two consecutive infections. J Clin Microbiol 25:1535–1539.

Ooi LS, Ho WS, Ngai KL, Tian L, Chan PK, Sun SS, Ooi VE. 2010. Narcissus Tazetta Lectin shows strong inhibitory effects against respiratory syncytial virus, influenza A (H1N1, H3N2, H5N1) and B viruses. J Biosci 35:95–103.

Oshansky CM, Zhang W, Moore E, Tripp RA. 2009. The host response and molecular pathogenesis associated with respiratory syncytial virus infection. Future Microbiol 4:279–297.

Parrott RH, Kim HW, Arrobio JO, Hodes DS, Murphy BR, Brandt CR, Camargo E, Chanock RM. 1973. Epidemiology of respiratory syncytial virus infection in Washington, D.C. II. Infection and disease with respect to age, immunologic status, race and sex. Am J Epidemiol 98:289–300.

Scott PD, Ochola R, Ngama M, Okiro EA, James Nokes D, Medley GF, Cane PA. 2005. Molecular analysis of respiratory syncytial virus reinfections in infants from Coastal Kenya. J Infect Dis 193:59–67.

Sullender WM, Mufson MA, Prince GA, Anderson LJ, Wertz GW. 1998. Antigenic and genetic diversity among the attachment proteins of group A respiratory syncytial viruses that have caused repeat infection in children. J Infect Dis 178:925–932.

Sullender WM. 2000. Respiratory syncytial virus genetic and antigenic diversity. Clin Microbiol Rev 13:1–15.

Waris M. 1991. Pattern of respiratory syncytial virus epidemics in Finland: Two-year cycles with alternating prevalence of groups A and B. J Infect Dis 163:464–469.

Welliver TP, Garofalo RP, Hosakote Y, Hintz KH, Avendano L, Sanchez K, Velozo L, Jafri H, Chavez-Bueno S, Ogra PL, McKinney L, Reed JL, Welliver RC Sr. 2007. Severe human lower respiratory tract illness caused by respiratory syncytial virus and influenza virus is characterized by the absence of pulmonary cytotoxic lymphocyte responses. J Infect Dis 195:1126–1136.

Yamaguchi M, Sano Y, Dapat IC, Saito R, Suzuki Y, Kumaki A, Shobugawa Y, Dapat C, Uchiyama M, Suzuki H. 2011. High frequency of repeated infections due to emerging genotypes of human respiratory syncytial viruses among children during eight successive epidemic seasons in Japan. J Clin Microbiol 49:1034–1040.

Yui I, Hoshi A, Shigeta Y, Takami T, Nakayama T. 2003. Detection of human respiratory syncytial virus sequences in peripheral blood mononuclear cells. J Med Virol 70:481–489.

Zhang W, Choi Y, Haynes LM, Harcourt JL, Anderson LJ, Jones LP, Tripp RA. 2010. Vaccination to induce antibodies blocking the CX3C–CX3CR1 interaction of respiratory syncytial virus G protein reduces pulmonary inflammation and virus replication in mice. J Virol 84:1148–1157.

Zlateva KT, Vijgen L, Dekeersmaeker N, Naranjo C, Van Ranst M. 2007. Subgroup prevalence and genotype circulation patterns of human respiratory syncytial virus in Belgium during ten successive epidemic seasons. J Clin Microbiol 45:3022–3030.

J Infect Chemother (2013) 19:480–485
DOI 10.1007/s10156-012-0515-3

ORIGINAL ARTICLE

Mumps Hoshino and Torii vaccine strains were distinguished from circulating wild strains

Akihito Sawada · Yoshiaki Yamaji · Tetsuo Nakayama

Received: 4 September 2012 / Accepted: 22 October 2012 / Published online: 9 November 2012

Abstract Aseptic meningitis and acute parotitis have been observed after mumps vaccination. Mumps outbreaks have been reported in Japan because of low vaccine coverage, and molecular differentiation is required to determine whether these cases are vaccine associated. RT-nested PCR was performed in the small hydrophobic gene region, and viruses were differentiated by restriction fragment length polymorphism assay. A total of 584 nucleotides were amplified. The PCR product of the Hoshino strain was cut into two fragments (313 and 271 nucleotides) by *Mfe*I; that of the Torii strain was digested with *Eco*T22I, resulting in 332- and 252-nucleotide fragments. Both strains were genotype B and had an *Xba*I site, resulting in two fragments: 299 and 285 nucleotides. Current circulating wild types were cut only by *Xba*I or *Mfe*I. However, the *Mfe*I site of the wild types was different from that of the Hoshino strain, resulting in 451- and 133-nucleotide fragments. Using three restriction enzymes, two mumps vaccine strains were distinguished from wild types, and this separation was applied to the identification of vaccine-related adverse events.

Keywords Mumps Hoshino strain · Mumps Torii strain · Molecular differentiation · Wild circulating genotypes

Introduction

In Japan, the MMR vaccine was introduced in 1989 but discontinued in 1993 because of an unexpectedly high incidence of aseptic meningitis caused by components of the mumps vaccine [1, 2]. The mechanisms responsible for the high incidence of aseptic meningitis with the MMR vaccine have not been elucidated in comparison to monovalent mumps vaccines used since 1993. Nagai et al. [3] investigated the incidence of aseptic meningitis after vaccination and identified 10 cases among 21,465 vaccine recipients. Moreover, 13 patients with aseptic meningitis were reported among 1,051 cases of naturally acquired mumps confirmed by viral isolation together with genome detection. The incidence of aseptic meningitis after vaccination was 1/27 of that observed for natural infections. However, in the post marketing study, the incidence of aseptic meningitis was approximately 0.01 % (1 case in 10,000 recipients) and that of acute parotitis, 2–3 %.

The mumps virus strains were divided into 12 genotypes based upon the sequence diversity of the small hydrophobic (SH) genome region [4, 5]. Parental strains of the Hoshino and Torii vaccine strains, isolated in the 1960s, are genotype B [6, 7]. Circulating wild-type strains were all genotype B in the 1970s and earlier and were genotypes J and B in the 1980s to 1990s. Genotype G appeared in the 2000s. Genotypes D, I, and L have been isolated sporadically [8–10], and recently genotype G was globally the major circulating genotype [11]. Large outbreaks have been observed every 3–5 years because of the low vaccine coverage, 30 % to 40 %. The mumps vaccine is voluntary (its cost is not covered by the government), and a guardian's decision usually depends on information on mumps outbreaks. Some recipients were immunized during the incubation period of natural infection, making it difficult to determine whether the mumps illness was caused by a natural infection or the vaccine.

In previous reports, the Hoshino vaccine strain was distinguished from circulating wild strains using the

A. Sawada · Y. Yamaji · T. Nakayama (✉)
Kitasato Institute for Life Sciences, Laboratory of Viral Infection I, 5-9-1 Shirokane, Minato-ku, Tokyo 108-8641, Japan
e-mail: tetsuo-n@lisci.kitasato-u.ac.jp